# Structural Microtubule Cap: Stability, Catastrophe, Rescue, and Third State

Imre M. Jánosi,*† Denis Chrétien,‡ and Henrik Flyvbjerg§

*The Niels Bohr Institute, DK-2100 Copenhagen Ø, Denmark; †Department of Physics of Complex Systems, Eötvös University, H-1117 Budapest, Hungary; ‡Equipe Structure et Dynamique du Cytosquelette, UMR 6026, Université de Rennes 1, F-35042 Rennes, France; and §Materials Research Department, Risø National Laboratory, DK-4000 Roskilde, Denmark

ABSTRACT Microtubules polymerize from GTP-liganded tubulin dimers, but are essentially made of GDP-liganded tubulin. We investigate the tug-of-war resulting from the fact that GDP-liganded tubulin favors a curved configuration, but is forced to remain in a straight one when part of a microtubule. We point out that near the end of a microtubule, the proximity of the end shifts the balance in this tug-of-war, with some protofilament bending as result. This somewhat relaxes the microtubule lattice near its end, resulting in a *structural cap*. This structural cap thus is a simple mechanical consequence of two well-established facts: protofilaments made of GDP-liganded tubulin have intrinsic curvature, and microtubules are elastic, made from material that can yield to forces, in casu its own intrinsic forces. We explore possible properties of this structural cap, and demonstrate 1) how it allows both polymerization from GTP-liganded tubulin and rapid depolymerization in its absence; 2) how rescue can occur; 3) how a third, meta-stable intermediate state is possible and can explain some experimental results; and 4) how the tapered tips observed at polymerizing microtubule ends are stabilized during growth, though unable to accommodate a lateral cap. This scenario thus supports the widely accepted GTP-cap model by suggesting a stabilizing mechanism that explains the many aspects of dynamic instability.

## INTRODUCTION

Microtubules (MTs) are self-assembling tubular polymers made of the protein tubulin. They are found in all eukaryotic cells, where they provide rigidity where needed in nature's designs. During mitosis they form a highly dynamic spindle, where individual MTs persistently grow or shrink by polymerization and depolymerization. The stochastic interconversion between the assembling and disassembling states is called *dynamic instability* (Mitchison and Kirschner, 1984; Walker et al., 1988), with the transition to depolymerization referred to as *catastrophe* and the transition back to polymerization referred to as *rescue*.

In vitro and in vivo, MTs polymerize from tubulin dimers liganded with two units of GTP (tubulin-t), but are essentially made of tubulin liganded with one unit of GTP and one unit of GDP (tubulin-d) (Desai and Mitchison, 1997). The difference is due to hydrolysis of one GTP to GDP shortly after incorporation of tubulin-t into the MT lattice (Caplow, 1992; Erickson and O'Brien, 1992). This hydrolysis supposedly causes a straight-to-curved configurational change of the dimer; this is indicated by polymerization studies in the presence of slowly hydrolyzable GTP analogs GMPPNP and GMPCPP (Kirschner, 1978; Mejillano et al., 1990; Hyman et al., 1995; Müller-Reichert et al., 1998). Bound as it is to its neighbor dimers in a closed MT, the curved configuration cannot be realized. Instead, the energy released by GTP hydrolysis is stored as stress in the MT's wall, and the hidden intrinsic curvature of its protofilaments poise the MT toward depolymerization (Caplow et al., 1994; Tran et al., 1997a). It is believed that a very short, so far unobserved (see, however, Drechsel and Kirschner, 1994) *cap* of freshly added tubulin-t at polymerizing MT ends is responsible for the stability of the tubule (Mitchison and Kirschner, 1984; Caplow and Shanks, 1996; Vandecandelacre et al., 1999). Alternatively, a *lateral* cap of GDP-$P_i$-liganded tubulin was proposed quite recently (Panda et al., 2002). GTP or GDP-$P_i$, whatever its difference to tubulin-t, loss of this cap is believed to trigger catastrophe. The protofilaments curling off the depolymerizing end of MTs amply display the intrinsic curvature that was hidden in the straight wall of the intact tube (Kirschner, 1978; Mandelkow and Mandelkow, 1985; Mandelkow et al., 1991; Tran et al., 1997a; Müller-Reichert et al., 1998).

In the present article we point out that near the end of an MT, the proximity of the end allows some relief of the built-in stress through slight protofilament bending. This idea stems from energy considerations for the relatively long protofilament sheets that sometimes terminate the plus end of growing MTs (Chrétien et al., 1995, 1999; Arnal et al., 2000). Such outwardly curved sheets are in a more relaxed state than the tube they decorate, so one may speculate whether they contribute to its stability (Jánosi et al., 1998; Chrétien et al., 1999). If they do, they cannot be crucial for stability because many MTs have *blunt* ends (Horio and Hotani, 1986; Walker et al., 1988).

In the present article we show that stress release does not require a complicated end structure. Blunt MT ends also lower their elastic energy by adopting a relaxed configura-

*Submitted January 25, 2002, and accepted for publication May 6, 2002.*

Address reprint requests to Henrik Flyvbjerg, PO Box 49, Roskilde DK-4000, Denmark. Tel.: 45-353-25285; Fax: 45-353-25016; E-mail: flyvbjerg@nbi.dk.



0006-3495/02/09/1317/14 $2.00

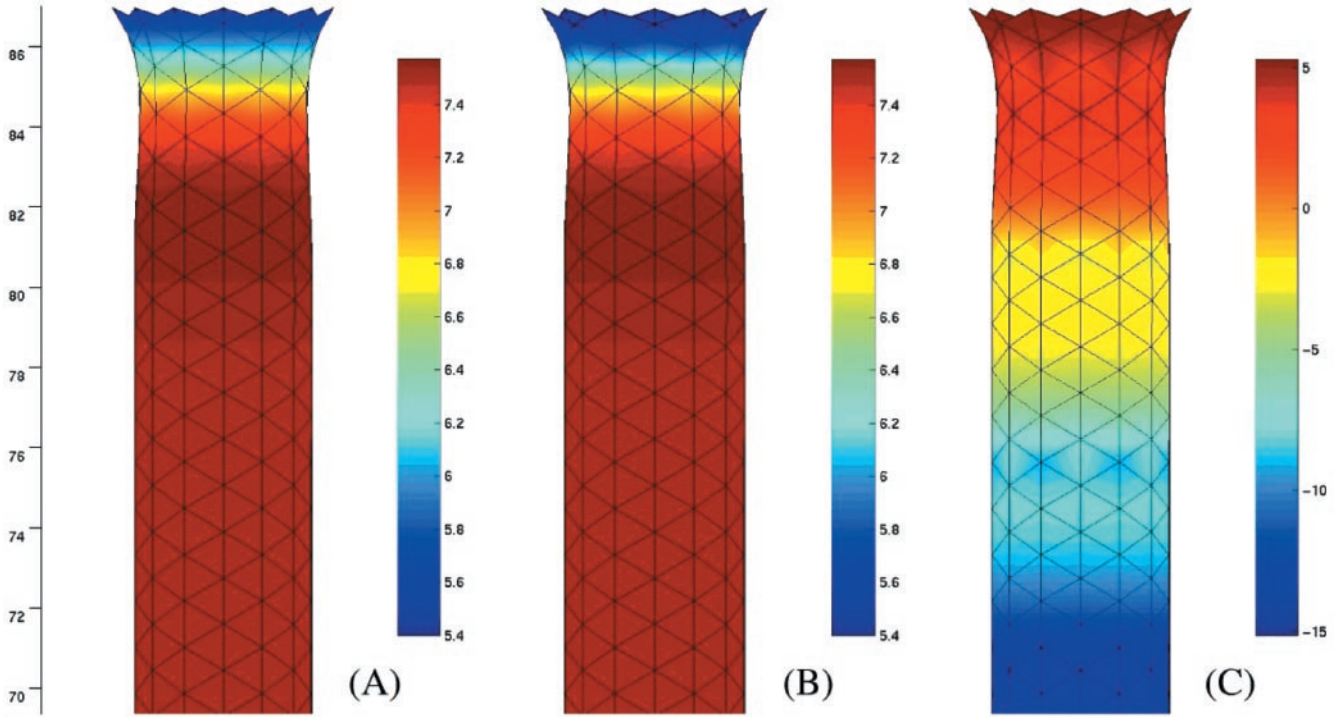


FIGURE 1 Homogeneous sheet of elastic material with built-in competing curvatures forming a tube with a blunt end. The material was computer-simulated as a triangulated surface and the energies stored locally in the surface are shown with color coding on a logarithmic scale. (*A*) Total energy density. (*B*) Longitudinal bending energy. (*C*) Transverse stretching energy. The zig-zag shape of the blunt end is an irrelevant artifact of the triangulation used.

tion, plus- and minus-ends alike. This local relaxation amounts to a *structural cap*, and does not depend on the presence of tubulin-t. It is a simple mechanical consequence of two well-established facts: 1) protofilaments made of tubulin-d have intrinsic curvature, and 2) MTs are elastic, made from material that yields to forces, including its own built-in stresses.

We explore properties of this structural cap, and demonstrate how it allows polymerization from tubulin-t and rapid depolymerization in the absence of tubulin-t. We describe a third, meta-stable intermediate state and explain some experimental results with it. We propose a mechanism for rescue, the least understood aspect of dynamic instability. We suggest how the tapered tips observed at polymerizing MT ends are stabilized during growth despite their inability to accommodate a lateral cap.

While tubulin-d is known to form protofilaments with built-in curvature, it is only a hypothesis that tubulin-t forms straight protofilaments. We explore the consequences of this hypothesis here. Those of our results that depend on properties of tubulin-t at all, depend only on the weaker hypothesis that tubulin-t forms protofilaments that prefer to be *more straight* than those formed from tubulin-d, so where we write "straight" below, one may substitute "straighter" and arrive at the same conclusions.

## MATERIALS AND METHODS

### Computer simulations

The main points of this paper do not rely on a detailed description of tubulin's structure, not even on a description of MTs in terms of protofilaments. We consider an MT a tube made from a sheet of elastic material that will stretch and bend, but resists doing this with a characteristic *stiffness* for each mode of deformation. The sheet has built-in curvatures: laterally, its intrinsic curvature is that of the tube itself; longitudinally, its intrinsic curvature is that observed in protofilaments peeling off depolymerizing MTs. The longitudinal intrinsic curvature of the sheet will bend it away from the symmetry axis of the tube if allowed to do so. Based on these general assumptions, we can formulate a simple sheet model that is universally valid for any tubular structure made from elastic material and having competing intrinsic curvatures. This model is described in details in Jánosi et al. (1998).

The preferred shape of an elastic sheet minimizes its total energy, which is a sum of contributions from stretching and bending terms. Although analytical calculations are possible for simple configurations (Jánosi et al., 1998), in general, numerical relaxation is needed to find energy-minimizing shapes, such as those shown in Fig. 1. Elastic parameters can be estimated by comparing simulated and measured curvatures for sheets, as well as computed and measured values for the flexural rigidity (Jánosi and Flyvbjerg, submitted for publication).

### Microtubule images

The cryoelectron microscope images used here, Fig. 6 below, were taken from Chrétien et al. (1995). Details concerning the preparation of samples and imaging conditions can be found in this reference.

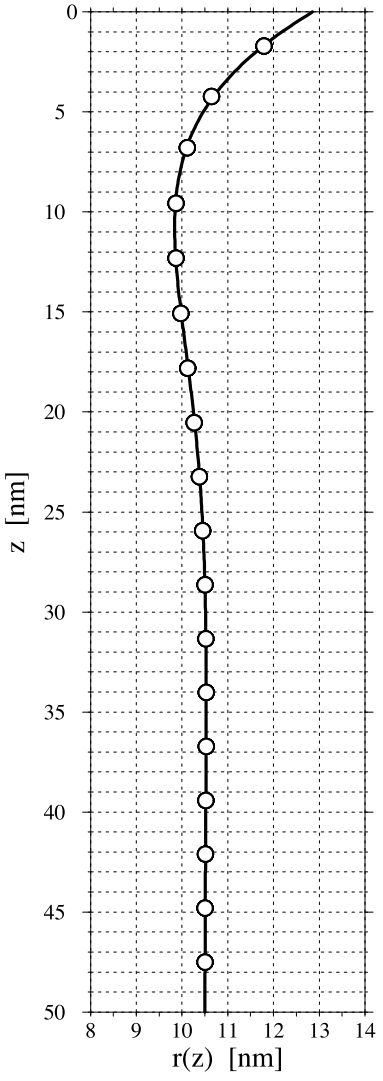


FIGURE 2 Fit of $r(z) = r_0 + \Delta r(z)$ as given in Eq. 7 (*solid line*) to the blunt end configuration shown in Fig. 1 (*circles*). The lengths are chosen to be typical for microtubules. For the sake of visualization, the figure is compressed vertically, as indicated by the mesh ($1 \times 1$ nm). The fit yielded $z_1/z_0 = -0.92$, not so different from the value obtained by minimizing the energy of the purely analytical model, $z_1/z_0 = -\pi/4 = -0.79$ in Eq. 11.

## Mathematical analysis: The filament model

Assuming the sheet material is uniform in its intrinsic properties, a blunt-ended MT is rotationally symmetric about its central axis—either fully so, or with respect to rotations that are integer multipla of $2\pi/13$, depending on whether we think of the MT wall as made from a continuous sheet, or from 13 laterally bound protofilaments running parallel with the MT axis. Both symmetries allow a simple characterization of the MT's shape. We shall find that this shape is not just a simple cylinder.

We consider a semi-infinite MT with coordinate $z$, $0 \le z < \infty$, denoting positions along its length; see Figs. 1 and 2. The elastic energy stored in a small part of the wall located at $z$ depends on the tube's diameter $r(z)$ and its longitudinal curvature $c(z)$ at $z$. In our analytical calculations we ignore longitudinal stretching and lateral bending in comparison with lateral stretching and longitudinal bending, because our computer simulations show that their role is negligible. This allows a simple one-dimensional analytical description of a thin stripe, or "filament," of the wall material.

### *Uniform tube*

The local longitudinal curvature $c(z)$ of a segment at distance $z$ from the MT end is

$$c(z) = \frac{d^2r}{dz^2}. \tag{1}$$

The associated bending energy density is assumed quadratic in the difference to the intrinsic curvature $c_0$,

$$E_c(z) = \tfrac{1}{2}\, a[c(z) - c_0]^2, \tag{2}$$

where $a$ is a material parameter, the material's stiffness (bending rigidity per unit length) toward changes in longitudinal curvature $c$ away from the material's intrinsic longitudinal curvature $c_0$.

Non-zero local curvature is possible only if the distance $r$ of the wall from the central MT axis varies with $z$, in which case the lateral "bonds" store a stretching energy per unit length equal to

$$E_s(z) = \tfrac{1}{2}\, k[r(z) - r_0]^2. \tag{3}$$

Here, $r_0$ is the equilibrium radius of the cylinder, and $k$ is the stretching coefficient. As already mentioned, and expanded on below, computer simulations show that the two other energy terms, for longitudinal stretching and lateral bending, are extremely small in the relevant parameter range. We consequently neglect them in the present analysis.

Ignoring longitudinal stretching and lateral bending, the total energy of the tube is the sum of only two contributions, but from all segments along the $z$-axis, of course:

$$E[r] = \int_0^\infty dz \left( \frac{1}{2}\, a \left( \frac{d^2r(z)}{dz^2} - c_0 \right)^2 + \frac{1}{2}\, k(r(z) - r_0)^2 \right), \tag{4}$$

For the sake of simplicity we have placed one end of the tube at infinity, because the solution for a long, finite tube with a clamped end at $z = L$, and $L$ much larger than the tube's diameter, is the same, essentially. In equilibrium, the functional derivative of the energy $\delta E/\delta r(z)$ must vanish, which results in the following fourth-order ordinary differential equation for the shape $r(z)$ (Lanczos, 1949):

$$a\, \frac{d^4r(z)}{dz^4} + k[r(z) - r_0] = 0. \tag{5}$$

Introducing $\Delta r(z) = r(z) - r_0$ results in:

$$\left[ \left( \frac{d}{dz} \right)^4 + \frac{k}{a} \right] \Delta r(z) = 0. \tag{6}$$

This equation is known as the "static beam equation" (Landau and Lifshitz, 1986). It describes the equilibrium shape of a thin rod under a distributed load. In our case, the load on a filament is due to its *prestressed* state, caused by competing intrinsic curvatures, and it can be expressed simply with the deviations from equilibrium distances and curvatures.

A unique solution to Eq. 6 is specified by four boundary conditions. Far from the blunt end, the equilibrium configuration is a straight cylinder, $\Delta r(\infty) = 0$ (equilibrium radius) and $\Delta r'(\infty) = 0$ (the tube is straight). The boundary conditions at $z = 0$ are free, hence must be found by energy

minimization. The general solution to Eq. 6 that satisfies the boundary conditions at $z = \infty$ has the form

$$\Delta r(z) = A \cos\left(\frac{z - z_1}{z_0}\right) e^{z/z_0} \tag{7}$$

with

$$z_0 = \left(\frac{4a}{k}\right)^{1/4}. \tag{8}$$

Here, the amplitude $A$ and phase $z_1$ are the two parameters to be determined by energy minimization. It is straightforward to substitute Ansatz 7 into Eq. 4 by noticing that $r'' \equiv \Delta r''$:

$$E(A, z_1) = \frac{A^2 k z_0}{4} - \frac{A c_0 a}{z_0}\left[\cos\left(\frac{z_1}{z_0}\right) - \sin\left(\frac{z_1}{z_0}\right)\right] + E_0. \tag{9}$$

Here $E_0 = \frac{1}{2}\, a c_0^2 \int_0^\infty dz$ is the elastic energy stored in the wall of a straight semi-infinite tube made from wall material with intrinsic curvature $c_0$. Energy minimization with respect to $A$ and $z_1$ is achieved by solving the stationarity conditions

$$\frac{\partial E(A, z_1)}{\partial A} = 0 \quad \text{and} \quad \frac{\partial E(A, z_1)}{\partial z_1} = 0 \tag{10}$$

simultaneously. After some algebra we have

$$A = c_0 \sqrt{\frac{2a}{k}} \quad \text{and} \quad z_1 = -\frac{\pi}{4} z_0, \tag{11}$$

$$E_{\min} = -\frac{1}{2} c_0^2 a z_0 + E_0. \tag{12}$$

### *Energy barrier toward depolymerization*

From the equations just solved, it follows that the end of a semi-infinite tube has a radius $r_{eq}(0) > r_0$, as shown in Figs. 1 and 2,

$$\Delta r_{eq}(0) = c_0 \sqrt{\frac{a}{k}}. \tag{13}$$

Because the lateral bonds between protofilaments in an MT can be stretched only a little before they break, it is of interest for us to calculate the energy connected with a forced increase of $r(0)$, or, equivalently, $\Delta r(0)$. The energy required to increase $r(0)$ to a value corresponding to the breaking point for lateral bonds is the energy required to initiate depolymerization of the MT in our simple model.

For any forced value of $\Delta r(0)$, we write the amplitude in Eq. 7 as $A = \Delta r(0)/\cos(z_1/z_0)$ and use this to replace $A$ in the energy Eq. 9 with $\Delta r(0)$. We then minimize the resulting energy with respect to the only free variable left, $z_1$, to find

$$z_1[\Delta r(0)] = z_0 \arctan\left(-\frac{c_0}{\Delta r(0)} \sqrt{\frac{a}{k}}\right), \tag{14}$$

and the corresponding minimal energy, which is just a second-degree polynomial,

$$E[\Delta r(0)] = \frac{k z_0}{4} \Delta r^2(0) - \frac{c_0 a}{z_0} \Delta r(0) - \frac{1}{4} a c_0^2 z_0 + E_0. \tag{15}$$

### *GTP contribution to cap*

In the framework of this mathematical filament model, a *GTP cap* is modeled as a finite segment of the same elastic material, but having *zero* intrinsic curvature. This segment "caps" a semi-infinite tube of tubulin-d, i.e., the material described above, having intrinsic curvature $c_0$.

The elastic energy of a tube capped by a finite straight segment of length $L$ is given by

$$E_{\text{tot}}(r) = \int_0^L dz \left\{\frac{1}{2} a \left[\frac{d^2 r(z)}{dz^2}\right]^2 + \frac{1}{2} k [r(z) - r_0]^2\right\} + \int_L^\infty dz [E_c(z) + E_s(z)], \tag{16}$$

where $E_c(z)$ and $E_s(z)$ are given by Eqs. 2 and 3 for the GDP-part spanning from $L$ to infinity, and the first term is for the GTP segment of zero intrinsic curvature, but of the same bending and stretching rigidity. The variational principle gives the same shape equation (6) as before (note that it does not contain $c_0$), thus the general solution Eq. 7 with Eq. 8 remains valid for the capped filament, too. The task is now to find the new $A^*$ and $z_1^*$ amplitude and phase parameters minimizing Eq. 16. The substitution gives the form

$$E(A^*, z_1^*) = \frac{A^{*2} k z_0}{4} - \frac{A^* c_0 a}{z_0} e^{-L/z_0}\left[\cos\left(\frac{z_1^* - L}{z_0}\right) - \sin\left(\frac{z_1^* - L}{z_0}\right)\right] + \frac{1}{2} a c_0^2 \int_L^\infty dz \tag{17}$$

in analogy with Eq. 9. The differences are the appearance of an exponential factor and phase shift in the second term, and the different integration range for the constant bending energy. From the minimization of Eq. 17 we get

$$A^* = c_0 \sqrt{\frac{2a}{k}}\, e^{-L/z_0} \quad \text{and} \quad z_1^* = -\frac{\pi}{4} z_0 + L. \tag{18}$$

The solutions for arbitrary end deflections can be obtained with the same method as described above. In analogy with Eq. 14 we get

$$z_1^*[\Delta r(0)] = z_0 \arctan\left(-\frac{c_0}{\Delta r(0)} \sqrt{\frac{a}{k}} \left(\cos\frac{L}{z_0} - \sin\frac{L}{z_0}\right) e^{-L/z_0}\right), \tag{19}$$

and the minimal energy as a function of end deflection, which also is just a second-degree polynomial:

$$E[\Delta r(0)] = \frac{kz_0}{4}\Delta r^2(0) - \frac{c_0 a}{z_0}\left(\cos\frac{L}{z_0} + \sin\frac{L}{z_0}\right)e^{-L/z_0}\Delta r(0) - \frac{1}{4}ac_0^2 z_0 e^{-2L/z_0}\left(1 - \sin\frac{2L}{z_0}\right) - \frac{1}{2}ac_0^2 L + E_0. \quad (20)$$

We shall analyze this expression in Fig. 5 below.

## RESULTS

### Theoretical results

Fig. 1 shows our main result: an effectively semi-infinite tube with a blunt end was allowed to relax (in a computer simulation) under the influence of its own internal forces. The parameters characterizing these forces were chosen as previously described (Chrétien et al., 1995; Jánosi et al., 1998) and in Jánosi and Flyvbjerg (submitted for publication), i.e., to reproduce the morphology of the long, curved sheets observed at the plus end of growing MTs (Chrétien et al., 1995) and the elastic properties of the tubes (Jánosi et al., 1998; Jánosi and Flyvbjerg, submitted for publication). The shape seen in Fig. 1 is a mathematically balanced compromise between stresses tending to bend the wall longitudinally, and resistance to lateral stretching of the same wall.

Now consider the stresses and energies stored in the configuration shown in Fig. 1. The color coding in Fig. 1 *A* shows the *total* local elastic energy stored in the wall. Well away from the end of the tube, this is just the energy difference between the longitudinally straight configuration of the material and its preferred longitudinally curved configuration, i.e., $E_0$ in Eq. 9. This scenario is closely analogous to that of an MT made from tubulin-d: *its* protofilaments also prefer to curve, but cannot do so except near the ends of the tube because they are laterally bound to each other, forming a one-protein thick sheet that forms a straight tube.

Near the end of the tube shown in Fig. 1 the most favorable configuration, i.e., the one with lowest mechanical energy, represents a compromise between the forces at play: the material bends somewhat, longitudinally, at the cost of stretching around the circumference. The net effect is a lower local energy stored in the tube, so in terms of local energy and geometry, this tube is capped by a structure different from its bulk: it displays a *structural cap*.

Fig. 1 *B* shows that the total energy density is dominated by longitudinal bending. The longitudinal curvature realized by the material also bends it *toward* the symmetry axis of the tube near the end of the tube (see Fig. 1 *B*, at heights below ~84, and, more clearly, Fig. 2 at $z < -12$ nm). This may seem counterintuitive, but it is a natural consequence of the mentioned tug-of-war: the wall can adopt locally unfavorable configurations to minimize the total energy.

Fig. 1 *C* shows the lateral stretching energy. It clearly increases toward the end, but its contribution to the total energy is at least one order of magnitude less than that of the longitudinal bending. If one imagines a limit to the material's lateral stretchability, a threshold beyond which the wall material tears, then depending on whether this threshold is higher or lower than the stretching seen in Fig. 1, the configuration shown is (meta-)stable or unstable. We elaborate this issue below.

We have not mentioned the longitudinal stretching energy or the lateral bending energy. They are there in the model as well, but turn out to be two to three orders of magnitude smaller than the longitudinal bending term, so they can be neglected to a very good approximation. Their small values can be understood as follows. When a *whole* MT is bent, longitudinal stretching and compression is the most important mode of deformation in terms of associated energy (Jánosi et al., 1998). Such bending induces some lateral bending, in the form of flattening of the tube's cross section, a response to bending that may lead to local buckling, but for an unbent and otherwise undisturbed MT like the one considered here, the primary deformation of the tube is longitudinal bending of protofilaments seeking their preferred curved shape, and not bending of the tube as such. Lateral stretching and bending are caused by this longitudinal bending, because longitudinal bending changes the local diameter of the tube. A change in diameter obviously causes lateral stretching or compression, but it also changes the lateral curvature, because the curvature is the inverse radius. It is the resistance to these two changes that limits the longitudinal bending of protofilaments. Lateral stretching/compression dominates this resistance, we find, with the parameter values determined in Jánosi et al. (1998) and Jánosi and Flyvbjerg (submitted for publication), so a tubulin sheet bends relatively easily laterally, but is difficult to compress/stretch. Most sheet materials share this property for the simple reason that bending is done by a combined stretching and compression of opposite sides of the material in a manner that makes the stiffness toward this deformation scale like the cube of the thickness, while the stiffness toward in-plane compression/stretching of the same sheet material scales like the thickness itself (Landau and Lifshitz, 1986; Howard, 2001). A *thin* piece of material typically bends easily, but may yet be difficult to stretch/compress: a common everyday experience with objects much larger than MTs.

Changes in the local diameter of the tube also cause a slight local longitudinal compression, as we find in our simulation. Again, the stiffness toward compression is relatively large; that is why MTs are stiff, so the role of this mode of deformation is negligible when we analyze the

shapes in Fig. 1: protofilaments function as incompressible struts under the deformations shown in Fig. 1. This is very easy to understand with the arguments just given for sheets in general. The primary force at play in Fig. 1 is the protofilaments' stiffness toward bending away from their intrinsic curvature, and this stiffness is much smaller than their stiffness toward compression. Then we expect to find very little compression, as we do.

The mathematical filament model described in Materials and Methods provides more insight into the energetics of the relaxed end-configurations. As a direct test of the filament model, we show in Fig. 2 how the shape function given in Eq. 7 fits the computer-simulated model, the blunt end shown in Fig. 1. Note that the function given in Eq. 7 is unique: it contains no free parameters, as its parameters are given in Eqs. 8 and 11. The discrete nature of the computer-simulated model requires us to fit the phase parameter $z_1$, however. That done, we see in Fig. 2 that the agreement between theory and simulation is excellent.

The shape in Fig. 2 represents a "zero-temperature" configuration, i.e., a configuration of minimal energy, with no thermal bending allowed for. In the case of real MTs, thermal forces bend whole tubes visibly (Mickey and Howard, 1995; Felgner et al., 1997). The modes of lowest bending energy are the global ones that vary slowly across the object. They are excited thermally with the largest amplitude.

We consider a slowly varying bending mode that changes $\Delta r(0)$ away from its equilibrium value, with the lowest possible increase in the elastic energy of the tube. We found the energy of this mode as in Materials and Methods.

The solutions are very similar to the equilibrium shape shown in Fig. 2. All shapes are harmonic oscillations with an amplitude that decreases exponentially with the distance to the end.

What interests us is the energy $E[\Delta r(0)]$ of the filament as a function of end deflection $\Delta r(0)$. It is given in Eq. 15 and its graph in Fig. 3. It is a simple quadratic form, increasing with $\Delta r(0)$ for $\Delta r(0) > \Delta r_{eq}(0)$ [see Eq. 13], until, at a critical value $\Delta r_{crit}(0)$, lateral bonds break and the liberated part of the filament rolls up to realize its intrinsic curvature $c_0$. Once started, bond breaking can continue if the geometric shape characterized by $\Delta r(0) = \Delta r_{crit}(0)$ can be sustained while it moves down the tube. If it can, the net effect is that the straight part of the tube is shortened and the amount it is shortened by is turned into separated, rolled-up protofilaments. This critical geometrical shape was created by a thermal fluctuation, but sustaining it during continued depolymerization plausibly requires that some of the energy released as a protofilament separates from the MT lattice and curls up, is transferred to the MT. The details of how this may happen is beyond our simple model, and its description is a project in its own right because it involves lateral bond-breaking and thermal energy gains and losses. However, the model does suggest a scenario: at finite temperatures the MT is meta-stable; once a thermal fluctuation has changed its shape to such an extent that lateral bonds break—at its end where this costs the least energy—bond-breaking may propagate down the tube, driven by the energy released by the curling up of intrinsically curved protofilaments. Conversely, if this energy release is not excessive, a thermal fluctuation just might *remove* enough energy from the end of the MT to relax the shape of its end from the depolymerizing critical state and back into the meta-stable state characterized by $\Delta r(0) < \Delta r_{crit}(0)$. Thus *rescue* may occur as the result of a random thermal fluctuation, just as catastrophes do in this scenario. If it does, it does so at a rate that increases with temperature, and this is indeed found experimentally (see Fig. 13 in Fygenson et al., 1994).

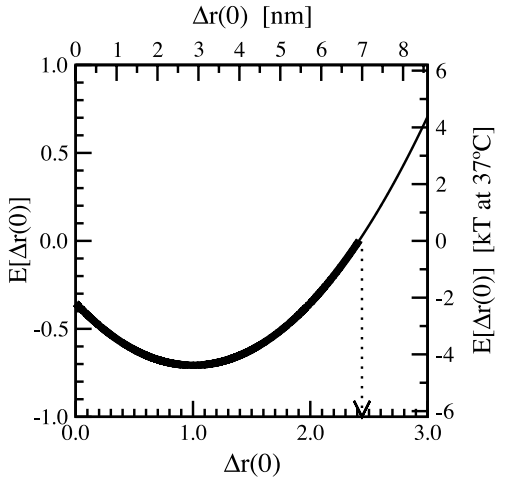


FIGURE 3 The elastic energy $E[\Delta r(0)]$ of the filament model relative to $E_0$ (in units of $ac_0^2 z_0/\sqrt{2}$ on the left axis; in units of $kT$ on the right axis), as a function of end deflection $\Delta r(0)$ (in units of $r_{eq}(0)$ on the bottom axis; in nanometers on the top axis). The vertical dotted line marks a hypothetical critical value for $\Delta r(0)$, beyond which lateral bonds break.

Now consider an MT with a GTP cap. We assume that tubulin-t has the same elastic properties (bending and stretching rigidities) as tubulin-d, but forms filaments that are intrinsically straight. The filament model was solved for the case of such a GTP cap of length $L$ in Materials and Methods.

Comparing the amplitudes $A$ and $A^*$ in Eqs. 11 and 18, we see that a GTP cap stabilizes an MT simply by being intrinsically straight, and it does this quite efficiently: exponentially in the cap size $L$ (see Fig. 4).

Fig. 5 shows the energy $E(\Delta r(0); L)$ of a filament as a function of end deflection $\Delta r(0)$, for various cap lengths $L$. The dashed line is the case of zero cap, also shown in Fig. 4. The dotted line shows the energy minimum with respect to $\Delta r(0)$ as a function of $L$. At very short cap lengths, the minimal energy increases with $L$, because outward bending of the terminal GDP segment is hindered by the GTP cap. The energy barrier toward depolymerization nevertheless increases with $L$ for all values of $L$.

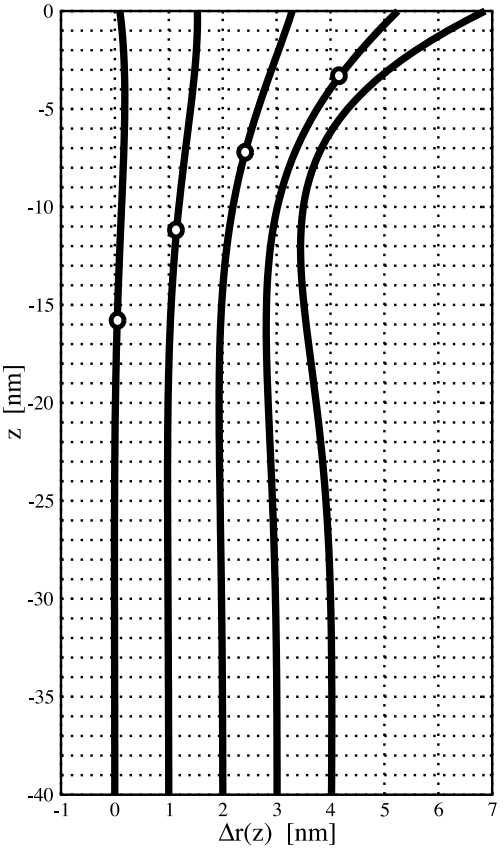


FIGURE 4 The effect of a finite straight cap on the end configuration. The elastic parameters are the same, the starting point of the cap is indicated with a circle. The rightmost filament has no cap. (It differs a little in shape from that in Fig. 2 because the latter was fitted to Fig. 1's simulated shapes.) The following filaments, from *right* to *left*, have caps of length 4 nm, 8 nm, 12 nm, and 16 nm. The curves have been shifted horizontally for a clear view.

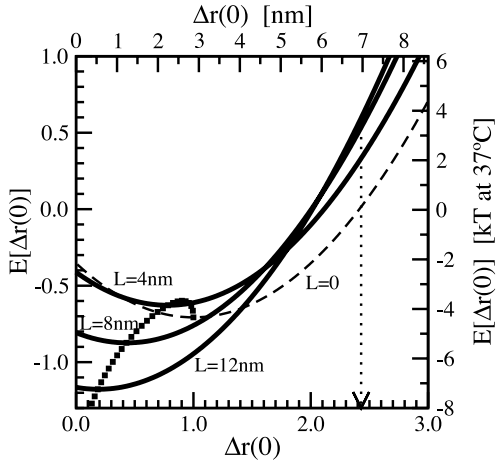


FIGURE 5 The elastic energy $E[\Delta r(0)]$ of a filament relative to the value $E_0$ takes in the case of no cap (in units of $ac_0^2 z_0/\sqrt{2}$ on the left axis; in units of $kT$ on the right axis) as a function of end deflection $\Delta r(0)$ (on bottom axis in units of the value of $r_{eq}(0)$ for case of no cap; on top axis in nanometers) for different cap lengths $L$. Heavy dots indicate the location of the energy minimum for various values of $L$. The vertical dotted line marks a hypothetical critical value for $\Delta r(0)$, beyond which lateral bonds break. The difference in energy between the minimal value and the value at the critical $\Delta r(0)$ is the energy barrier towards depolymerization. As expected, it is seen to grow with the cap length $L$, even though lateral bond strengths are assumed to be the same for cap and bulk of the microtubule.

## Comparing theory with experimental results

To compare our findings with observations of MT ends, we estimate the extent of the deformations expected at the end of a real MT. Our model cannot provide an accurate value by itself. It only restricts parameters to a certain range (Jánosi and Flyvbjerg, submitted for publication). An estimate can be obtained from data in Chrétien and Fuller (2000), which presents a comprehensive experimental analysis of energetically unfavorable MT configurations. The main result is that the tubulin lattice can tolerate distortions due to unfavorable protofilament number and/or different helical pitch, and does this by compression or elongation of intra and intermolecular bonds. Some distortions result in a longitudinal shift of protofilaments relatively to each other, observed as a changed subunit rise. Other distortions result in an altered protofilament separation (see Fig. 3 and Table 2 in Chrétien and Fuller, 2000).

While the longitudinal shift might be associated with a reorganization in the complex lateral bonding structure (Nogales et al., 1999), an increased protofilament separation (with subunit-rise close to its equilibrium value) is more naturally associated with an elastic deformation in the lateral direction. No configurations were observed that would correspond to $>\sim 0.2$ nm lateral stretching per tubulin subunit. It may be that bonds can tolerate larger strains, but the point we want to make here and now is that an elongation of 0.2 nm has been observed in lateral bonds. This corresponds to a 4% increase in perimeter when all the lateral bonds around the tube are stretched. The latter situation allows maximal outward bending of a blunt MT end, and a corresponding 4% or $\sim 0.5$ nm increase in the MT radius right at its end. This value is close to what can be resolved experimentally, if not below. (Note that shorter distances can be accurately measured in a *periodic* structure by means of Fourier or Moiré analysis, but the determination of end configurations requires direct observations.) The situation is even worse with respect to possible observation, if we include a possible GTP-cap in our considerations, because it reduces outward bending, as illustrated in Fig. 4).

In Fig. 6 we show some images of seemingly blunt MT ends from an ensemble in which most MTs were in a growing state. Despite our estimate above, most of these blunt ends display visible outward bending at the terminal rim, so maybe our model is correct, but our estimate above is not: maybe lateral bonds can tolerate more stretching without breaking than the 2 Å of our estimate, or maybe they cannot for tubulin-d, for which the estimate was done,

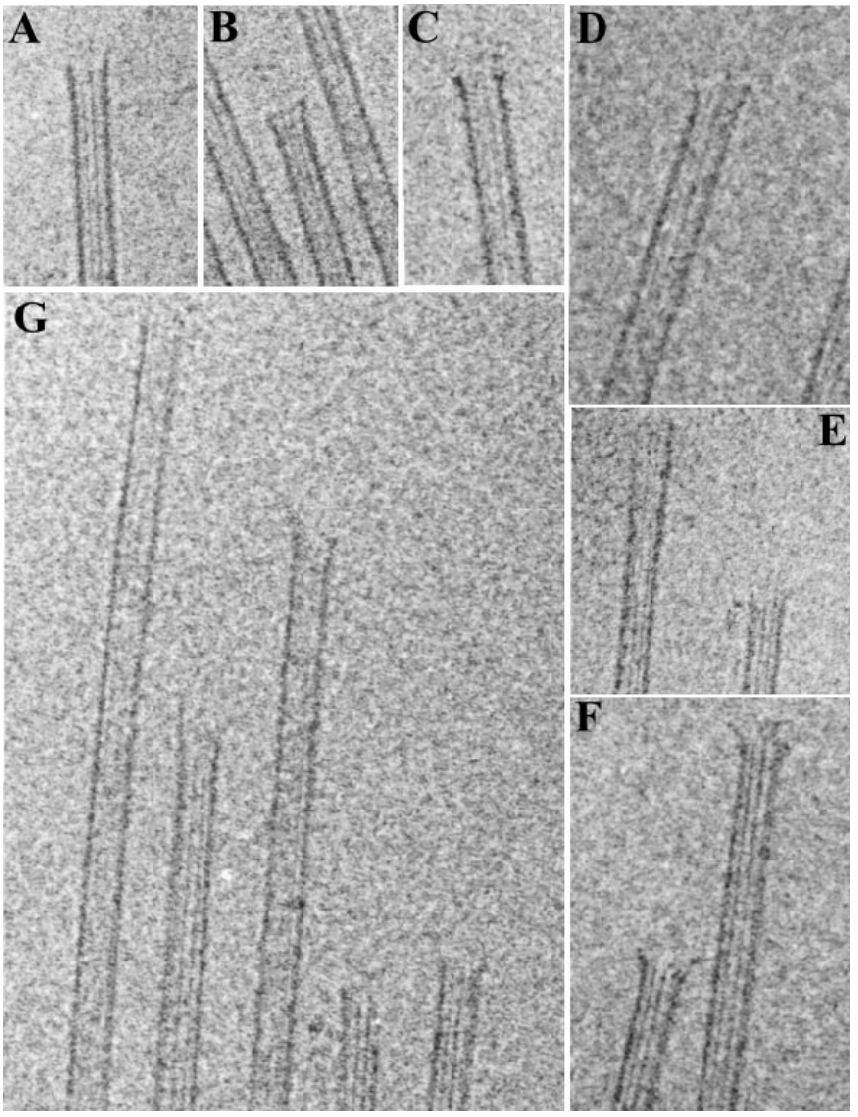


FIGURE 6 Electron micrographs of blunt microtubule ends. Different images have slightly different magnifications for better space filling. A length scale can be derived from a nominal MT diameter of 25 nm for 13-protofilament MTs (see text).

but can for tubulin-t. The latter is all that we need in order to see what we see in Fig. 6 with our model.

For each MT shown in Fig. 6 we have measured the diameter of its end, $d_{\text{end}}$, and, at several points along the body of the tube, the diameter of the body, $d_{\text{body}}$. This was done by counting pixels in a much-enlarged version of the plates in Fig. 6. Results for $d_{\text{body}}$ were averaged for precision for the individual tube. Tubes with 13 protofilaments were identified by their characteristic property of having protofilaments parallel to the MT axis. This property shows as two parallel dark lines in the center of the image, or no lines at all, according to whether four protofilaments overlap two and two in the projection where the image is, or precisely do not overlap.

Setting the diameter of the 13 pft body equal to 25 nm, we have $\Delta r(0) = d_{\text{end}}/(2d_{\text{body}}) \times 25$ nm. We found the following values for $\Delta r(0)$ in Fig. 6, measured in nanometers: *A*: 1.5 (13 pfts); *B*: 2.8 (13 pfts); *C*: 2.3; *D*: 3.5; *E*: left MT end is tapered, right MT end has protofilament attached; *F*: 6.7 (13 pfts) and 7.4 (13 pfts); *G*: left-to-right: 1.5, 1.5, 2.2 (12 pfts?), NA, and 2.5 (13 pfts). The MT-ends in plate *F* and the fourth end in plate *E* appear to have curled-up protofilaments attached to them, an indication that they are depolymerizing and should be disregarded. The remaining ends have $\Delta r(0)$ in an interesting range. For comparison, Figs. 4 and 5 show that our theory predicts $\Delta r(0) = 1.3$ nm for a cap consisting of a single straight dimer per protofilament, and $\Delta r(0) = 2.7$ nm for an MT with no cap. At this point it is worth noting that the parameters in our theory were determined long before we analyzed the plates in Fig. 6, and from quite different MT ends.

Fig. 4 also shows that the slight narrowing of the MT that occurs just before the widening at its end is negligible in the case of an MT with an 8 nm cap. Such a narrowing is also absent in Fig. 6, but this agreement proves nothing more than consistency, of course.

In view of the approximations built into our theory, the agreement between theory and experiment is so good that one interpretation of Fig. 6 is that it is showing the structural cap. The quantitative agreement we have found is what we would expect if this interpretation is correct. This is because the theory's parameters were chosen to make it fit observed MT ends which, by being tapered or ending in long sheets, displayed the curvature of the sheet material in such a clear manner that the parameters could be found (Jánosi et al., 1998).

The following alternative interpretation of Fig. 6 is also possible, however: maybe the ends observed are not really blunt, but terminate in very short curved sheets. The fact that the MT lattice is helical, hence must terminate in a somewhat jagged end, invites this interpretation.

Whatever the actual configuration of the MT end is, our key point is valid: a free end of an MT, be it blunt or tapered, is in a lower energy state than the body of the tube, because the protofilaments can relieve stress by bending a little in a manner that is not possible in the body of the tube. Furthermore, we have demonstrated that this stress relief at a free MT end is strongly enhanced by a cap of material in an intrinsically straight state, even a very short cap, and even a laterally incomplete cap: a few isolated tubulin-t dimers at a free MT end also help stabilize it; even a single tubulin-t dimer does.

## DISCUSSION

The ingredients in our structural cap model are not new. The integration of these ingredients in a three-dimensional scenario that makes it possible to analyze their interplay, is new. Our description provides a simple, plausible, and common mechanism for 1) the stabilizing effect of a GTP-cap that is short, or even incomplete; 2) the "third state," in which an MT neither grows nor depolymerizes; and 3) *rescue*, the phenomenon that an MT can change back from the depolymerizing state to the polymerizing state. We now discuss these aspects of our model and relate them to results in the literature when we can, and when no clear conclusions can be drawn.

### Persistent growth

Microtubule polymerization in vitro is a far-from-equilibrium reaction that depends strongly on temperature and the concentration of free tubulin (Walker et al., 1988; Erickson and O'Brien, 1992; Fygenson et al., 1994). Polymerization proceeds by addition of GTP-liganded tubulin to the end of an MT (Desai and Mitchison, 1997). During, or soon after, intersubunit bonds have been formed, the unit of GTP liganded to $\beta$-tubulin is hydrolyzed and inorganic phosphate is released.

Three important aspects should be emphasized here. First, GTP-liganded tubulin, the polymerizing dimer, prefers to be in a *straight* configuration, or a configuration *straighter* than the one preferred by GDP-liganded tubulin (Kirschner, 1978; Mejillano et al., 1990; Müller-Reichert et al., 1998), hence it must be assumed to be in that configuration while in solution and, consequently, when entering the MT lattice. Second, GTP hydrolysis is not necessary for polymerization to proceed. Tubulin liganded with slowly hydrolyzable GTP-analogs also polymerize (Hyman et al., 1992; Drechsel and Kirschner, 1994). Third, GTP hydrolysis occurs very soon after the incorporation of a fresh subunit in the MT (Stewart et al., 1990; Walker et al., 1991; Melki et al., 1996), and GTP hydrolysis keeps pace with the addition of tubulin at various rates (Vandecandelacre et al., 1999). It is consequently believed that the GTP-cap must be *very short* (Caplow and Shanks, 1996), and a simple mechanism has been proposed that ensures this, while agreeing quantitatively with available experimental data (Flyvbjerg et al., 1994, 1996). Recent results obtained with a radiolabeling strategy yield that the cap is short indeed, consisting of one dimer per protofilament end; a dimer of tubulin-GDP-$P_i$, and not tubulin-GTP (Panda et al., 2002), but that makes no difference in our structural cap model.

These three properties (the polymerizing unit is straight(er); it needs not hydrolyze for polymerization to proceed; the cap is short) are all fully incorporated into our model: short, intrinsically straight(er) segments at the end of protofilaments result in an MT end with reduced outward longitudinal curvature, hence more stability toward catastrophe. For simple geometric reasons, such straight(er) end segments also favor formation of lateral bonds between any new straight(er) subunits that may be added; the subunits attach (more) parallel to each other, rather than pointing in different directions. Obviously, straight(er) segments need not turn into curved ones for more straight(er) segments to be added. On the contrary, MT made from protofilaments that are intrinsically straight(er) throughout their length are more stable than other MTs. They will only grow, and will not suffer catastrophe, according to our model.

This last point is in agreement with several experiments that suggest that addition of straight(er) subunits supports persistent growth and stability. MTs assembled in the presence of the stabilizing agent taxol (Arnal and Wade, 1995) and GMPCPP (Hyman et al., 1992, 1995; Müller-Reichert et al., 1998) have a longitudinal subunit spacing that exceeds that of GDP-liganded tubuling by $\sim$0.3 nm per unit tubulin. This indicates a straighter configuration, as explicitly shown by Müller-Reichert et al. (1998). Also, the XMAP215/TOGp family seems to keep straight the end of protofilaments, thus stimulating assembly and stabilizing MTs (Spittle et al., 2000). These results all support the hypothesis that GTP-tubulin is straight (or straighter than GDP-tubulin) and that this matters for polymerization. With an Oscar Wilde-pastiche he might have scorned, they point to "the importance of being straight."

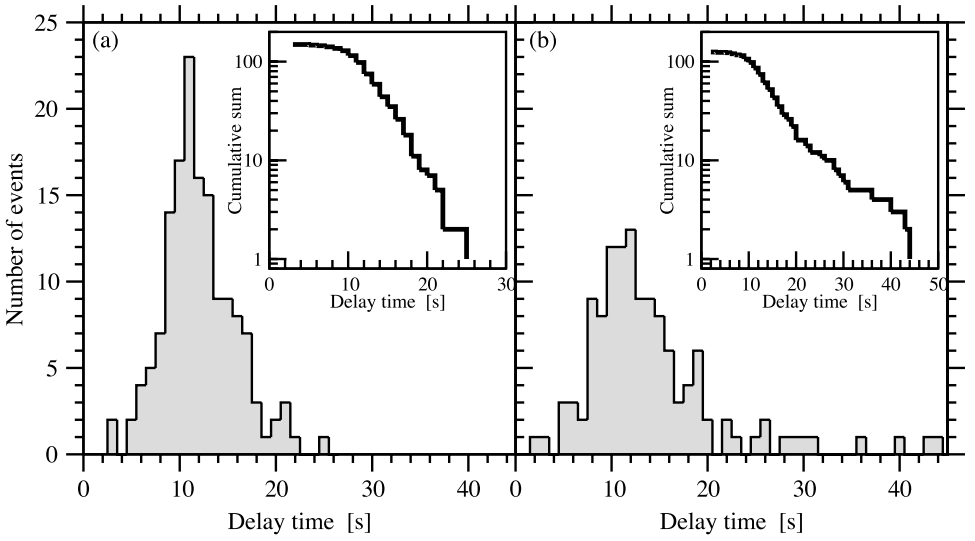


FIGURE 7 Histogram of the waiting time before catastrophes for the plus (*a*), and minus (*b*) ends. The *insets* show the cumulative distributions (from right to left) on a semilogarithmic scale. Data are from Walker et al. (1991).

## Catastrophes and "Third State"

Our cap model has as a logical consequence that a transition from the polymerizing state to the depolymerizing one, so-called *catastrophe*, occurs in two steps, via a third, quiescent state. In this, it is consistent with the proposal of Tran et al. (1997b) complementing the original cap model postulated by Mitchison and Kirschner (1984; see review by Desai and Mitchison, 1997). The first step is the loss of all GTP-liganded tubulin at the end. This may happen as a random event during growth, by GTP hydrolysis catching up with the addition of fresh units of GTP-liganded tubulin. It may be prompted in an experiment as described in Walker et al. (1991), by flushing out the tubulin-t-containing buffer and replacing it with buffer containing no tubulin-t, so that GTP hydrolysis quickly removes the GTP cap. Either way, the MT end is left in the meta-stable state we described above, a state which it leaves for the depolymerizing state only when a random thermal excitation pushes it over the energy barrier toward depolymerization. This third state, quiescent inasmuch as neither polymerization nor depolymerization occurs, has been observed directly by monitoring the length of an MT as function of time (Tran et al., 1997b; Vorobjev et al., 1997; Waterman-Storer and Salmon, 1997b; Odde et al., 1999; Quarmby, 2000).

Observation of its existence does not reveal its nature, but statistics for its "decay" to the depolymerizing state do. Because we propose this to occur by thermal barrier crossing, it follows that the waiting time for it to occur is stochastic and *exponentially distributed*, just like that of radioactive decay. One consequence of this exponential distribution is that the root-mean-square deviation (=standard deviation) of the waiting time distribution equals the mean waiting time. This property, as well as the exponential distribution itself, should be observable, if this last step is the "bottleneck" in the two-step process to catastrophe. Conversely, if losing the tubulin-t units at the MT end is the bottleneck, the statistics of the second step drown in the statistics of the first, resulting in a two-step process that looks effectively as a one-step process.

According to observations, the latter seems to be the situation when catastrophes are studied in *growing* MTs. The continued addition of fresh tubulin-t units at the growing end makes the loss of these units the bottleneck, but in experiments where growth is arrested by flushing out the tubulin-t-containing buffer, the "GTP cap" is quickly lost by hydrolysis, and the second step is optimally observable. Fig. 7 shows statistics for such an experiment. In practice, it is difficult to say exactly when growth is arrested for the individual MT observed, because it takes a few seconds to flush the chamber in which the experiment is done. Once growth has been arrested, loss of the GTP cap is also a stochastic process. But if it is not the bottleneck, then most GTP caps are gone from an ensemble of MT ends after a few average lifetimes for GTP caps under these circumstances, and additional waiting times are exponentially distributed. Such an exponential distribution is clearly seen for delay times larger than 10 s in the inset in Fig. 7 *a*, i.e., for plus ends. The inset for minus ends in Fig. 7 *b* appears to show the sum of two exponentials, one dropping off faster than the other, with one dominating between 10 and 20 s, and the other dominating after 20 s, though the statistics are not good in this case. These two exponentials are what one would see if the population of MTs studied consisted of two "species" with different barriers toward depolymerization. Clearly, if two different MT lattice configurations are predominant in a population, they constitute such two species according to our scenario for the transition from the third state to the depolymerizing state.

The exponential delay time distributions shown in Fig. 7 have characteristic times of 3 and 5 s for panels *a* and *b*,

respectively, and the tail showing after 20 s in panel *B* has a characteristic time of 12 s. Can we relate these experimental numbers to properties of our model? The answer is yes and no. Yes, if we add one more feature to our model; no, if we don't. We can identify the inverse of the characteristic time with the reaction rate $k$, the reaction being the transition form the third state to the depolymerizing state. Then we can apply classical reaction-rate theory in which the Van't Hoff-Arrhenius law gives the rate in terms of a threshold energy for activation, $E_b$,

$$k = \nu \exp(-E_b/(k_B T)) \tag{21}$$

where $k_B$ is Boltzmann's constant and $T$ the absolute temperature (Hänggi et al., 1990). The threshold energy is provided by our model, $E_b = E(\Delta r_{crit}(0)) - E(\Delta r_{eq}(0))$, so our model gives the temperature dependence of the rate and predicts classical Arrhenius behavior, but our model does not give the dimensional prefactor $\nu$, which is needed to obtain a result at a given temperature. To determine $\nu$, one needs more information about the transition state than our model offers. One may extend our model by detailing the transition state to the degree required to obtain $\nu$. That does not lead to a prediction of the experimental rate, it only integrates the information contained in the experimental rate into the model by extending the latter.

The temperature dependence of the time a growing microtubule will grow before catastrophe occurs has been measured at various tubulin concentrations; (see Fig. 12 *A* in Fygenson et al., 1994). It increases with increasing temperature, while Eq. 21 describes a decrease with temperature (an increase in the rate). Equation 21 does not describe the catastrophe rate, however, but only the second step in the two-step process to catastrophe that we propose. The first step, loss of cap, is suppressed by increasing temperature, because higher temperature causes faster polymerization. Therefore, our theory is not inconsistent with experimental data, but also receives no support on this point.

Fig. 12 *B* in Fygenson et al. (1994) offers the sought support when combined with Fig. 12 *A*, however. At a fixed MT velocity of growth, the time until catastrophe is longer at lower temperatures. It is a good deal more temperature-dependent than the rate in Eq. 21, but then the first step, the loss of cap through GTP hydrolysis, is also slowed at lower temperature, we imagine. Theory and experiment are consistent with each other. The catastrophe frequency as a function of growth rate at different temperatures shows the behavior we expect for a thermally activated process: the higher the temperature at the same growth rate, the higher the catastrophe frequency (see Fig. 9 in Fygenson et al., 1994).

Aspects of the scenario presented here—that the stability of an MT tip is partly mechanical in origin, and that catastrophes are two-stage processes with a thermally driven second stage—have simple consequences we must address. First of all, GTP hydrolysis is believed to induce a local conformational change near the dimer interface (Downing and Nogales, 1998). This change must have a mechanical effect at *both* MT ends, and catastrophes indeed occur at both ends in vitro (Horio and Hotani, 1986; Walker et al., 1988). This they do with different kinetic parameters, however (Walker et al., 1988, 1989, 1991; Tran et al., 1997b). Our simple model does not describe details of the complex bond between adjacent tubulin subunits (Nogales et al., 1999), and consequently cannot explain *differences* between the dynamics of the two MT ends. Nogales (1999) hypothesizes that the lateral contacts between $\alpha$-tubulins (capping the negative end) can be stronger than between $\beta$ subunits having GDP at the nucleotide site. We could add such an effect in our model, and thus obtain different dynamics for the two ends, but this would be an ad hoc addition, hence lead to no additional insight.

The complexity of the protein-protein bonds and the sensitivity to subtle details is clearly demonstrated by a recent experiment in which deuterium oxide was found to suppress catastrophes very efficiently (Panda et al., 2000). Similar fine details can be responsible for the observed high variability in the rate of assembly and disassembly of individual MTs (Drechsel et al., 1992; Gildersleeve et al., 1992; Chrétien et al., 1995; Billger et al., 1996; Desai and Mitchison, 1997). This also is beyond our simple model, unless it is caused by differences in MT lattice structure. Different protofilament numbers would lead to different stability properties of MT ends even in our simple model.

Another simple consequence of our model is that if more stress is stored in the MT lattice near an MT end, a higher frequency of catastrophes results. Comparing to the equilibrium MT configuration (13 protofilaments, 3-start helix), an excess elastic energy can be stored by incorporating lattice defects or by forming a tubule with different protofilament numbers and different helicities of the lattice. Measurements of catastrophe frequencies as a function of protofilament number have not been done. The distributions of MT protofilament numbers and MT lengths in an ensemble have, however, been correlated with an enhanced catastrophe propensity: the distribution of MTs peaked very sharply near the 13.3 configuration in Chrétien and Fuller (2000) and supports such a correlation.

Alternatively, the elastic energy stored in the wall can be decreased by incorporating straight elements, as, e.g., in mixed GMPCPP-GDP or GTP-GDP lattices. Wild-type yeast MTs can contain 6% GTP-tubulin distributed in the wall (Dougherty et al., 1998). We believe that the stability of the MT's very end determines catastrophe probabilities. Consequently, we expect that MTs polymerized from a *mixture* of tubulins including a small percentage of straight elements will not show dramatically different stability toward catastrophe, a hypothesis that one can check experimentally. (Once catastrophe has occurred, however, such a

mixed-lattice MT will depolymerize only until a cap is encountered embedded in the lattice.)

Finally, it is well known that many agents in the buffer increase the frequency of catastrophe. These agents are not necessary for dynamic instability, however, because this phenomenon occurs also in purified tubulin solution (Desai and Mitchison, 1997). This supports that catastrophe really is an intrinsic capacity of the MT lattice, as we have described it, and the role of various agents is only to change the parameter values for properties on which this capacity depends, such as bond strengths and the flexibility/stiffness of tubulin.

## More about the third state

Direct experimental evidence for the existence of a stabilizing cap is based on the removal of the growing end (Mitchison and Kirschner, 1984; Keates and Hallett, 1988; Walker et al., 1989, 1991; Voter et al., 1991; Caplow, 1992; Tran et al., 1997b). To explain the results, in particular the observed waiting time between a cut and its consequences—usually depolymerization of plus ends, and growth at minus ends—Tran et al. (1997b) introduced the notion of a meta-stable *third state*. The existence of such a state-of-waiting is even more pronounced in vivo, where the new ends presumably arose by breaking of MTs under motor forces (Vorobjev et al., 1997; Waterman-Storer and Salmon, 1997b; Odde et al., 1999), or katanin (Quarmby, 2000). In our model, this third state occurs naturally at both MT ends that are created when an MT is cut. Figs. 1 and 2 illustrate that an MT end made from GDP-tubulin alone, like the MT ends created by cutting an MT, is meta-stable in our scenario. Its configuration is less stable than one involving straight segments of tubulin-t, so it has a higher probability per unit time for suffering catastrophe (cf. Fig. 5).

The very different behavior of the two MT ends created by cutting an MT we "explain" as due to the polarity of the tubulin dimer, hence beyond our simple model. We predict that in the absence of free GTP-tubulin in solution, the two MT ends created by a cut will suffer catastrophe at rather similar rates, just like the MT ends studied in dilution experiments (Voter et al., 1991; Walker et al., 1991).

## Rescue

Our model also suggests a specific mechanism for *rescue*, the transition from the depolymerizing to the polymerizing state. It suggests that rescue is caused by a random thermal fluctuation. At a typical physiological temperature an MT experiences thermal fluctuations; it even bends thermally. However, it is in the nature of thermal equilibrium that thermal fluctuations not only add configurational energy, they can and do remove it as well, and both processes occur at random. This rescue mechanism is then random, and intrinsic to MTs at physiological temperatures.

Experimentally, rescue does seem an intrinsic property of MT dynamics because it occurs in the absence of MT-associated proteins and other additives (Billger et al., 1996). It also appears to occur at random when MT-associated proteins are absent. Finally, it seems a thermally activated process, as we suggest, judging from its temperature dependence in Fig. 13 in Fygenson et al. (1994). Nevertheless, it is perhaps the least understood aspect of dynamic instability (Desai and Mitchison, 1997).

An alternative scenario for rescue goes as follows. As we mentioned above, fast depolymerization is plausibly driven by the spontaneous curling up of protofilaments (Tran et al., 1997a). However, long coiled oligomers remain attached only when they are stabilized by $Mg^{2+}$ or $Ca^{2+}$ ions (Mandelkow et al., 1991; Tran et al., 1997a). This suggests that breaking of longitudinal bonds in curled-up protofilaments occurs in parallel with their curling up. If the breaking of longitudinal bonds in a peeling protofilament is random and can happen at a position that has not crossed the energy barrier toward depolymerization (see Fig. 3), depolymerization ceases, the third state has been recovered, and a transition back to the growing state has become possible. Here, we have argued as if what happens to one protofilament, happens to all protofilaments in a tubule simultaneously. This is of course not the case. A real rescue requires that the overwhelming majority of protofilaments stop to shrink almost simultaneously. If we assume that the random breaking of longitudinal inter-dimer bonds is uncorrelated between protofilaments, this breaking must happen very often at links of subcritical deflection to arrive at a reasonable value for the joint probability. If lateral bond-breaking, however, is strongly correlated with the curling-up, e.g., triggered by it, and curling up occurs with the same speed for all protofilament (Tran et al., 1997a), coordinated by interactions via lateral bonds, then rescues are easily explained as occurring via the randomly recurring third state. Occam's razor clearly favors our first suggestion above, that rescue is the result of a simple thermal fluctuation relaxing the MT lattice from its depolymerizing state and into its meta-stable state.

Be that as it may, many details at the microscopic level remain to be clarified experimentally. On the theoretical side, full exploitation of our model regarding rescues requires a Monte Carlo simulation of it, treating each protofilament independently and accounting for its lateral bonds in the MT, and random breaking of longitudinal bonds as it curls up at a depolymerizing end. More experimental input is needed to guide the choices that must be made in the detailing of such a simulation.

Experimental support for the random nature of rescue just described would be provided by observation of pauses during depolymerization in a buffer without free tubulin. Such pauses we would interpret as the MT end being in the third

state. As no free tubulin is present, full rescue to the growing state cannot occur; but half the process, its first step, would have been observed in this interpretation. Such discontinuous shrinking is observed in various experiments (Gildersleeve et al., 1992; Caplow and Shanks, 1996; Vorobjev et al., 1997). The interpretation of these experiments is ambiguous, however, as the effect on the rescue process of solute tubulin and drugs present is not known.

### Tapered MT ends

Many MTs appear to grow as a sheet of laterally bound protofilaments that elongates at its tip, while closing into a tube at its base (Erickson, 1975; Simon and Salmon, 1990; Chrétien et al., 1995; Hyman and Karsenti, 1996; O'Toole et al., 1999; Arnal et al., 2000). GTP hydrolysis is not related to tubular geometry, it is observed also in extended flat sheets induced by zinc ions (Melki and Carlier, 1993) and in taxol-stabilized oligomers (Melki et al., 1996). This, and the absence of observable tubulin-t at growing MT ends, suggest that the curved terminal sheets are formed mostly from GDP tubulin, and only the very end of them can contain GTP subunits. The tubulin lattice in these open sheets does not experience the stresses that the lattice in closed tubules does, however. The sheets relax some of their elastic stresses by adopting a curved configuration, bending out longitudinally while bending toward closure into a tube laterally. (Jánosi et al., 1998; Chrétien et al., 1999). Such a sheet is consequently more stable in the third, meta-stable state than a closed tube is, and it is more effectively stabilized by a little tubulin-t at the ends of its protofilaments. It may consequently serve as a structural cap, further stabilized by tubulin-t. This scenario is quite far from that of a GTP-cap stabilizing the blunt ends of a MT like the hoops holding a barrel together, but it is logically consistent, and in agreement with observations.

I.M.J. thanks the Danish Research Agency's Graduate School of Biophysics at the Niels Bohr Institute for hospitality during the completion of this article, and the Hungarian National Science Foundation (OTKA) for support under Grant T032437. D.C. thanks the Fondation pour la Recherche Médicale and Ligue Nationale Contre le Cancer for their support.

## REFERENCES

Arnal, I., E. Karsenti, and A. A. Hyman. 2000. Structural transitions at microtubule ends correlate with their dynamic properties in *Xenopus* egg extracts. *J. Cell. Biol.* 149:767–774.

Arnal, I., and R. H. Wade. 1995. How does taxol stabilize microtubules? *Curr. Biol.* 5:900–908.

Billger, M. A., G. Bhatacharjee, and R. C. Williams, Jr. 1996. Dynamic instability of microtubules assembled from microtubule-associated protein-free tubulin: neither variability of growth and shortening rates nor "rescue" requires microtubule-associated proteins. *Biochemistry.* 35: 13656–13663.

Caplow, M. 1992. Microtubule dynamics. *Curr. Opin. Cell. Biol.* 4:58–65.

Caplow, M., R. L. Ruhlen, and J. Shanks. 1994. The free energy for hydrolysis of a microtubule-bound nucleotide triphosphate is near zero: all of the free energy for hydrolysis is stored in the microtubule lattice. *J. Cell Biol.* 127:779–788.

Caplow, M., and J. Shanks. 1996. Evidence that a single monolayer tubulin-GTP cap is both necessary and sufficient to stabilize microtubules. *Mol. Biol. Cell.* 7:663–675.

Caudron, N., O. Valiron, Y. Usson, P. Valiron, and D. Job. 2000. A reassessment of the factors affecting microtubule assembly and disassembly *in vitro*. *J. Mol. Biol.* 297:211–220.

Chrétien, D., and S. D. Fuller. 2000. Microtubules switch occasionally into unfavorable configurations during elongation. *J. Mol. Biol.* 298: 663–676.

Chrétien, D., S. D. Fuller, and E. Karsenti. 1995. Structure of growing microtubule ends: two-dimensional sheets close into tubes at variable rates. *J. Cell. Biol.* 129:1311–1328.

Chrétien, D., I. M. Jánosi, J. C. Taveau, and H. Flyvbjerg. 1999. Microtubule's conformational cap. *Cell Struct. Funct.* 24:299–303.

Desai, A., and T. J. Mitchison. 1997. Microtubule polymerization dynamics. *Annu. Rev. Cell. Dev. Biol.* 13:83–117.

Dougherty, C. A., R. H. Himes, L. Wilson, and K. W. Farrell. 1998. Detection of GTP and $P_i$ in wild-type and mutated yeast microtubules: implications for the role of the GTP/GDP-$P_i$ cap in microtubule dynamics. *Biochemistry.* 37:10861–10865.

Downing, K. H., and E. Nogales. 1998. Tubulin and microtubule structure. *Curr. Opin. Cell. Biol.* 10:16–22.

Drechsel, D. N., A. A. Hyman, M. H. Cobb, and M. W. Kirschner. 1992. Modulation of the dynamic instability of tubulin assembly by the microtubule-associated protein tau. *Mol. Biol. Cell.* 3:1141–1154.

Drechsel, D. N., and M. W. Kirschner. 1994. The minimum GTP cap required to stabilize microtubules. *Curr. Biol.* 4:1053–1061.

Erickson, H. P. 1975. The structure and assembly of microtubules. *Ann. N.Y. Acad. Sci.* 253:60–77.

Erickson, H. P., and E. T. O'Brien. 1992. Microtubule dynamic instability and GTP hydrolysis. *Annu. Rev. Biophys. Biomol. Struct.* 21:145–166.

Felgner, H., R. Frank, J. Biernat, E. M. Mandelkow, E. Mandelkow, B. Ludin, A. Matus, and M. Schliwa. 1997. Domains of neuronal microtubule-associated proteins and flexural rigidity of microtubules. *J. Cell. Biol.* 138:1067–1075.

Flyvbjerg, H., T. E. Holy, and S. Leibler. 1994. Stochastic dynamics of microtubules: a model for caps and catastrophes. *Phys. Rev. Lett.* 73: 2372–2375.

Flyvbjerg, H., T. E. Holy, and S. Leibler. 1996. Microtubule dynamics: caps, catastrophes, and coupled hydrolysis. *Phys. Rev. E.* 54:5538–5560.

Fygenson, D. K., E. Braun, and A. Libchaber. 1994. Phase diagram of microtubules. *Phys. Rev. E.* 50:1579–1588.

Gildersleeve, R. F., A. R. Cross, K. E. Cullen, A. P. Fagen, and R. C. Williams, Jr. 1992. Microtubules grow and shorten at intrinsically variable rates. *J. Biol. Chem.* 267:7995–8006.

Hänggi, P., P. Talkner, and M. Borkovec. 1990. Reaction-rate theory: fifty years after Kramers. *Rev. Mod. Phys.* 62:251–341.

Horio, T., and H. Hotani. 1986. Visualization of the dynamic instability of individual microtubules by dark-field microscopy. *Nature.* 321: 605–607.

Howard, J. 2001. Mechanics of Motor Proteins and the Cytoskeleton. Sinauer Associates, Inc., Sunderland, MA.

Hyman, A. A., D. Chrétien, I. Arnal, and R. H. Wade. 1995. Structural changes accompanying GTP hydrolysis in microtubules: information from a slowly hydrolyzable analogue guanylyl-($\alpha,\beta$)-methylene-diphosphonate. *J. Cell. Biol.* 128:117–125.

Hyman, A. A., and E. Karsenti. 1996. Morphogenetic properties of microtubules and mitotic spindle assembly. *Cell* 84:401–410.

Hyman, A. A., S. Salser, D. N. Drechsel, N. Unwin, and T. J. Mitchison. 1992. Role of GTP hydrolysis in microtubule dynamics: information from a slowly hydrolyzable analogue, GMPCPP. *Mol. Biol. Cell.* 3:1155–1167.

Jánosi, I. M., D. Chrétien, and H. Flyvbjerg. 1998. Modeling elastic properties of microtubule tips and walls. *Eur. Biophys. J.* 27:501–513.

Keates, R. A., and F. R. Hallett. 1988. Dynamic instabilities of sheared microtubules observed by quasi-elastic light scattering. *Science.* 241: 1642–1645.

Kirschner, M. W. 1978. Microtubule assembly and nucleation. *Int. Rev. Cytol.* 54:1–71.

Lanczos, C. 1949. The Variational Principles of Mechanics. University of Toronto Press, Toronto, Canada.

Landau, L. D. and E. M. Lifshitz. 1986. Theory of Elasticity, 3rd Ed. Pergamon Press, New York.

Mandelkow, E. M., and E. Mandelkow. 1985. Unstained microtubules studies by cryo-electron microscopy. Substructure, supertwist, and disassembly. *J. Mol. Biol.* 181:123–135.

Mandelkow, E. M., E. Mandelkow, and R. A. Milligan. 1991. Microtubule dynamics and microtubule caps: a time resolved cryo-electron microscopy study. *J. Cell. Biol.* 114:977–991.

Mejillano, M. R., J. S. Barton, and R. H. Himes. 1990. Stabilization of microtubules by GTP analogues. *Biochem. Biophys. Res. Commun.* 166:653–660.

Melki, R., and M. F. Carlier. 1993. Thermodynamics of tubulin polymerization into zinc sheets: assembly is not regulated by GTP hydrolysis. *Biochemistry.* 32:3405–3413.

Melki, R., S. Fievez, and M. F. Carlier. 1996. Continuous monitoring of $P_i$ release following nucleotide hydrolysis in actin or tubulin assembly using 2-amino-6-mercapto-7-methylpurine ribonucleoside and purine-nucleoside phosphorylase as an enzyme-linked assay. *Biochemistry.* 35:12038–12045.

Mickey, B., and J. Howard. 1995. The rigidity of microtubules is increased by stabilizing agents. *J. Cell. Biol.* 130:909–917.

Mitchison, T., and M. W. Kirschner. 1984. Dynamic instability of microtubule growth. *Nature.* 312:237–242.

Müller-Reichert, T., D. Chrétien, F. Severin, and A. A. Hyman. 1998. Structural changes at microtubule ends accompanying GTP hydrolysis: information from a slowly hydrolyzable analogue of GTP, guanylyl ($\alpha,\beta$)methylenediphosphonate. *Proc. Natl. Acad. Sci. U.S.A.* 95: 3661–3666.

Nogales, E. 1999. A structural view of microtubule dynamics. *Cell. Mol. Life. Sci.* 56:133–142.

Nogales, E., M. Whittaker, R. A. Milligan, and K. H. Downing. 1999. High-resolution model of the microtubule. *Cell* 96:79–88.

Odde, D. J., L. Cassimeris, and H. M. Buettner. 1995. Kinetics of microtubule catastrophe assessed by probabilistic analysis. *Biophys. J.* 69: 796–802.

Odde, D. J., L. Ma., A. H. Briggs, A. DeMarco, and M. W. Kirschner. 1999. Microtubule bending and breaking in living fibroblast cells. *J. Cell. Sci.* 112:3283–3288.

O'Toole, E. T., M. Winey, and J. R. McIntosh. 1999. High-voltage electron tomography of spindle pole bodies and early mitotic spindles in the yeast. *Mol. Biol. Cell.* 10:2017–2031.

Panda, D., G. Chakrabarti, J. Hudson, K. Pigg, H. P. Miller, L. Wilson, and R. H. Himes. 2000. Suppression of microtubule dynamic instability and treadmilling by deuterium oxide. *Biochemistry.* 39:5075–5081.

Panda, D., H. P. Miller, and L. Wilson. 2002. Determination of the size and chemical nature of the "cap" at microtubule ends using modulators of polymerization dynamics. *Biochemistry.* 41:1609–1617.

Quarmby, L. 2000. Cellular samurai: katanin and the severing of microtubules. *J. Cell. Sci.* 113:2821–2827.

Simon, J. R., and E. D. Salmon. 1990. The structure of microtubule ends during the elongation and shortening phases of dynamic instability examined by negative-stain electron microscopy. *J. Cell Sci.* 96: 571–582.

Spittle, C., S. Charrasse, Ch. Larroque, and L. Cassimeris. 2000. The interaction of TOGp with microtubules and tubulin. *J. Biol. Chem.* 275:20748–20753.

Steinmetz, M. O., R. A. Kammerer, W. Jahnke, A. Lustig, and J. van Oostrum. 2000. Op18/stathmin caps a kinked protofilament-like tubulin tetramer. *EMBO J.* 19:572–580.

Stewart, R. J., K. W. Farrell, and L. Wilson. 1990. Role of GTP hydrolysis in microtubule polymerization: evidence for a coupled hydrolysis mechanism. *Biochemistry.* 29:6489–6498.

Tran, P. T., P. Joshi, and E. D. Salmon. 1997a. How tubulin subunits are lost from the shortening ends of microtubules. *J. Struct. Biol.* 118: 107–118.

Tran, P. T., R. A. Walker, and E. D. Salmon. 1997b. A metastable intermediate state of microtubule dynamic instability that differs significantly between plus and minus ends. *J. Cell. Biol.* 138:105–117.

Vandecandelacre, A., M. Brune, M. R. Webb, S. R. Martin, and P. M. Bayley. 1999. Phosphate release during microtubule assembly: what stabilizes growing microtubules? *Biochemistry.* 38:8179–8188.

Vorobjev, I. A., T. M. Svitkina, and G. G. Borisy. 1997. Cytoplasmic assembly of microtubules in cultured cells. *J. Cell. Sci.* 110:2635–2645.

Voter, W. A., E. T. O'Brien, and H. P. Erickson. 1991. Dilution-induced disassembly of microtubules: relation to dynamic instability and the GTP cap. *Cell. Motil. Cytoskel.* 18:55–62.

Walker, R. A., S. Inoué, and E. D. Salmon. 1989. Asymmetric behavior of severed microtubule ends after ultraviolet-microbeam irradiation of individual microtubules in vitro. *J. Cell. Biol.* 108:931–937.

Walker, R. A., E. T. O'Brien, N. K. Pryer, M. F. Soboeiro, W. A. Voter, H. P. Erickson, and E. D. Salmon. 1988. Dynamic instability of individual microtubules analyzed by video light microscopy: rate constants and transition frequencies. *J. Cell. Biol.* 107:1437–1448.

Walker, R. A., N. K. Pryer, and E. D. Salmon. 1991. Dilution of individual microtubules observed in real time in vitro: evidence that cap size is small and independent of elongation rate. *J. Cell. Biol.* 114:73–81.

Waterman-Storer, C. M., and E. D. Salmon. 1997a. Treadmilling comes around again. *Curr. Biol.* 7:R369–R372.

Waterman-Storer, C. M., and E. D. Salmon. 1997b. Actomyosin-based retrograde flow of microtubules in the lamella of migrating epithelial cells influences microtubule dynamic instability and turnover and is associated with microtubule breakage and treadmilling. *J. Cell. Biol.* 139:417–434.

Wiese, Ch., and Y. Zheng. 2000. A new function for the γ-tubulin ring complex as a microtubule minus-end cap. *Nat. Cell. Biol.* 2:358–364.